

Carbon-Based Materials/Latex Composite from *Euphorbia Tirucalli* Plant for Potential Bone Fracture Treatment

Supardi^{1a}, Pranita Wardani^{2a}, and Wipsar Sunu Brams Dwandaru^{3a*}

Abstract: This study aims to investigate the preparation and characterization of carbon-based materials (CMs)/latex composites from the *Euphorbia tirucalli* plant for potential bone fracture treatment. The primary objectives are to: i) determine the antibacterial property of the CMs/latex composites against *Staphylococcus aureus* bacteria; and ii) determine the tensile strength of the CMs/latex composites via chicken bones as the model. The CMs were prepared using a simple heating method, using an oven at a temperature of 250 oC. The CMs/latex composites were prepared by mixing 3 ml of the latex and CMs solutions with concentrations of 10%, 20%, and 40% in 10 ml of distilled water. The CMs were characterized using UV-Vis, PL, and FTIR spectroscopies. The antibacterial property and tensile strength of the CMs/latex composites were tested using the diffusion method and an ultimate testing machine, respectively. The results obtained demonstrate that the CMs had absorption and emission peaks at wavelengths of 287 nm and 499 nm, respectively, resulting in cyan luminescence. The FTIR test of the CMs indicated the existence of the C=C, O-H, and N=C=S functional groups. The CMs/latex composites produced the highest diameter of inhibition zone and tensile strength of 3.24 mm and 0.02 kN, respectively. These findings show the potential application of CMs/latex composites for bone fracture treatment with antibacterial properties.

Keywords: CMs, CMs/latex composites, bone fracture treatment, *Euphorbia tirucalli* plant.

1. Introduction

Euphorbia tirucalli (*E. tirucalli*) has been known as an herbal plant, especially in Asian countries (da Silva et al., 2022). Various parts of the *Euphorbia* plant, such as its latex, stems, and twigs, have certain benefits, especially in traditional and/or herbal medicine. In various Asian countries, this plant is claimed to have many benefits for treating various diseases, e.g., cancer (Mali & Panchal, 2017). *Euphorbia* latex can treat fractures and accelerate wound healing, while the twigs can reduce bone and nerve pains (da Silva et al., 2022; Maver et al., 2015). The latex comes out from the surrounding branches that have been cut. Although latex is claimed to be able to treat fractures, research on this is relatively rare. The branches of the *Euphorbia* plant contain flavonoids and tannins, which produce anti-bacterial activity and potentially prevent wound infections (Pallavali et al., 2019). The latex and stem extracts from *E. tirucalli* were tested as antimicrobials against *Staphylococcus aureus* (*S. aureus*), *Bacillus subtilis* (*B. subtilis*), and *Pseudomonas aeruginosa* (*P. aeruginosa*) bacteria (Mali & Panchal, 2017). Moreover, converting the unused parts of the plant into carbon-based materials (CMs) may increase the applicability of the *Euphorbia* plant.

CMs hold a critical role in the development of functional materials. CMs include graphite, graphene and its derivatives, fullerene, carbon nanotubes (CNTs), biochar, and carbon nanodots (Cdots) (Sabzehmeidani et al., 2021; Liu et al., 2020). For example, Cdots are 0-dimensional (0D) nanomaterials with sizes

of 1 nm to 10 nm. They comprise carbon atoms as the core and functional groups such as carbonyl, carboxyl, hydroxyl, or amine as the surface state (Xia et al., 2019). They are favorable to be mass produced because they have novel properties, e.g., good solubility, strong luminescence, biocompatibility, and non-toxicity (Kaur & Verma, 2022; Ghosh et al., 2022). CMs, especially Cdots, can be prepared from various organic carbon precursors, viz.: nam-nam fruit (Dwandaru et al., 2020), Arabic gum (Thakur et al., 2014), guar gum (Rahmani & Ghaemy, 2019), latex of *E. mili* (Bano et al., 2019), and also wastes such as watermelon peel (Liu et al., 2016) and chicken bone (Dwandaru & Sari, 2020). Various preparation methods can produce CMs: Hummer's method (Sabzehmeidani et al., 2021), hydrothermal (Khajuria et al., 2018; Bano et al., 2019; Dwandaru et al., 2019), microwave (Baipai et al., 2019; Pires et al., 2015; de Medeiros et al., 2019), pyrolysis (Weber & Quicker, 2018), and carbonization at low temperatures (Liu et al., 2016).

CMs have been widely utilized for various applications, including biosensors, photocatalysts, drug delivery systems, antibacterial agents, heat and power production, and soil amendment (Zhai et al., 2012; Wang & Hu, 2017; Weber & Quicker, 2018). For some examples, Cdots have been used for antibacterials with conjunctions to other antimicrobial reagents, such as H₂O₂, Na₂CO₃, and AcOH (acetic acid) (Dong et al., 2017). Cdots can help antimicrobial reagents to inhibit bacterial activities. In addition, N-doped Cdots/hydroxyapatite nanocomposites have also been developed for bone repair. Adding Cdots significantly improves bone regeneration and repair (Khajuria et al., 2018; Shao et al., 2017). Furthermore, C-dots can be conjugated with latex

Authors information:

^aPhysics Education Department, Faculty of Mathematics and Natural Sciences, Universitas Negeri Yogyakarta, Jl. Colombo No. 1, Karangmalang, Yogyakarta, 55281, INDONESIA. E-mail: supardi@uny.ac.id¹; ranita.anita2016@student.uny.ac.id²; wipsarian@uny.ac.id³

*Corresponding Author: wipsarian@uny.ac.id

Received: September, 2023

Accepted: June 20, 2024

Published: June, 2025

materials, such as XSBR, which can be used as nano-filters (Sreenath et al., 2020).

The handling of bone fractures is typically carried out using plates, pins, wires, and couplers. The problem is that these objects are metals, foreign objects in the body. The use of plates and couplers requires drilling the bone. In this study, we offer another alternative in treating bone fractures using CMs from *E. tirucalli* as an additive for the fracture treatment. The chicken bone is used as a model for the bone fracture. The *E. tirucalli* latex is mixed with the CMs to form a CMs/latex composite. The characteristics of the resulting CMs are examined using ultraviolet-visible (UV-Vis) spectrophotometry, photoluminescence (PL) spectroscopy, and Fourier transform infrared (FTIR) spectroscopy. The tensile strength of the CMs/latex composites applied to the chicken bone is examined using the universal testing machine (UTM). The antibacterial properties of the CMs and CMs/latex composites based on the diameter inhibition zone (DIZ) against *S. aureus* bacteria are also determined.

This study explores the potential of a composite material, i.e., CMs/latex, for bone fracture treatment. There are limited studies in the related literature on applying *E. tirucalli* for bone fracture treatment. Furthermore, the combination of CMs and *E. tirucalli* latex has not been extensively investigated. By assessing the antibacterial properties and mechanical strength of this composite material, this study contributes to the development of bone fracture treatment. This study highlights its approach, interdisciplinary relevance, and potential contribution to advancing CMs and healthcare. It offers a novel and interdisciplinary investigation at the crossroads of CMs and medicine. It addresses the utilization of *E. tirucalli*-derived CMs and *E. tirucalli* latex in treating bone fractures, which has seen limited exploration thus far. By combining the inherent antibacterial properties of *E. tirucalli* with the advanced

properties of CMs, we aim to develop a composite material with enhanced mechanical strength and antibacterial properties, providing a potential alternative to conventional approaches in bone fracture treatment.

The antibacterial ability of the CMs/latex composites provides a safe treatment of bone fractures and prevents infection when applied to the bones. Moreover, the improved tensile strength of the CMs/latex composites provides a better and safer support and/or buffer in the healing process of the bone fracture. Hence, the specific objectives of this study are i) to determine the antibacterial property of the CMs/latex composites against *S. aureus* bacteria; and ii) to determine the tensile strength of the CMs/latex composites via chicken bones as the model bones. The CMs produced in this study, their incorporation into latex, antibacterial assessments, and mechanical testing on a chicken bone model, offer a comprehensive examination of the composite's potential efficacy. In this case, the chicken bones are used as a real-life model for bones. Of course, the chicken bones used in this study do not respond to the treatment, as no living cells exist. However, in this study we do not directly investigate the respond of the bones to the treatment and leave this for future studies. In addition to its immediate applications in medicine, the findings of this study could hold broader implications for the advancement of CMs and their tailored use in medical contexts.

2. Method

The latex was extracted from the *E. tirucalli* plant. This was conducted by cutting the branches of the *E. tirucalli* plants. The latex came out drop by drop from the ends of the cut branches. The latex was collected into a container and tightly sealed to prevent drying. This process can be observed in Figure 1.

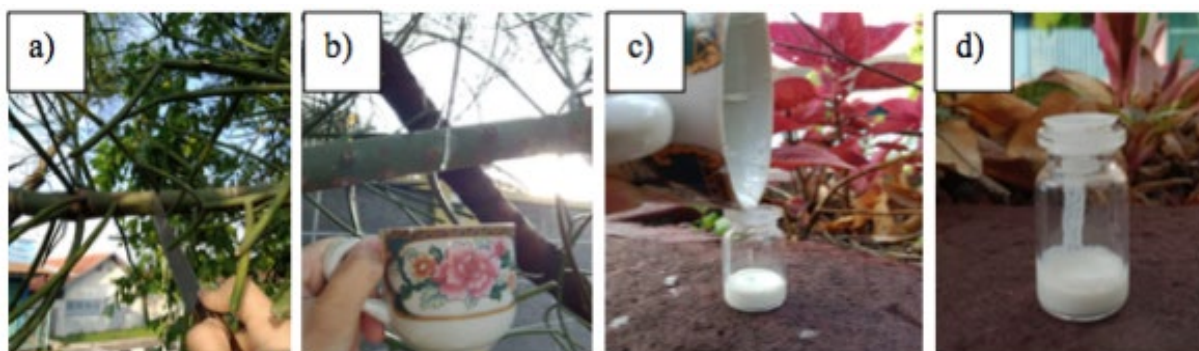


Figure 1. Latex collection of the *E. tirucalli* plant, i.e., a) cutting the branches; b) collecting the latex in a cup, c) pouring the latex into a sample container, and d) tightly sealing the latex in the sample container.

The CMs were prepared by washing 50 grams of *E. tirucalli* branch wastes, then cutting them into small pieces. Next, the branches were dried in the sun for 6 hours. The branches were heated in a Mitseda Electric Oven at a temperature of 250 °C for 2 hours and then mashed into powder. The powder was filtered to ensure that the powder size was homogeneous. The oven is heated to 250 °C for 20 minutes. The powder was then dissolved

in distilled water at a ratio of 1:1, stirred, and left alone for 24 hours. The solution was then filtered twice using a 110 μm filter paper. Hence, the CMs solution was produced.

The CMs were characterized using a UV-Vis spectrophotometer, a PL spectrometer, and an FTIR spectrometer. The UV-Vis (Shimadzu 2450 Series) spectrophotometer was used to determine the wavelengths at the absorption peaks of the CMs.

The PL spectrometer was self-assembled using an Ocean Optics USB 4000 Fiber Optic spectrometer and a laser (405 nm) source to determine the emission wavelength produced by the CMs. Finally, an FTIR (Thermo Nicolet Avatar 360 IR) spectrometer was employed to identify the functional groups produced by the CMs.

The CMs/latex composite was prepared by mixing 10 ml of distilled water, 3 ml of latex solution, and CMs solution with

concentrations of 10%, 20%, and 40%. Then, the mixture was heated and stirred to obtain CMs/latex solution with a sticky texture and white color. Hence, three samples of CMs/latex composites were produced, i.e., CMs/latex A, B, and C for 10%, 20%, and 40% CMs concentrations, respectively (Figure 2).

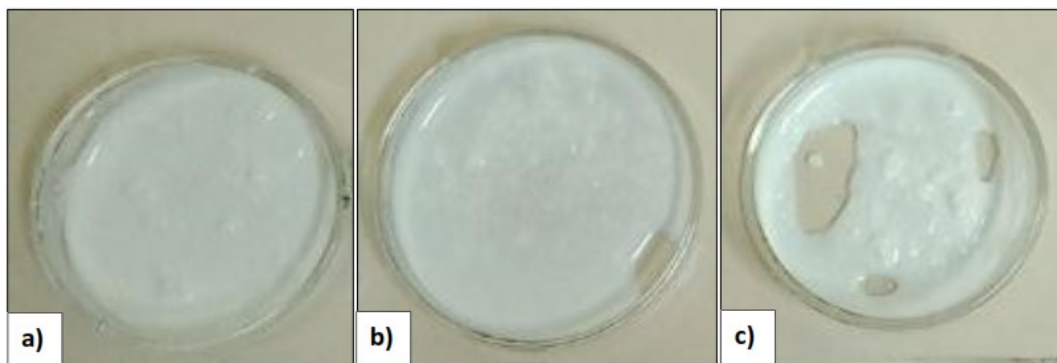


Figure 2. Samples of CMs/latex composites of (a) A, (b) B, and (c) C.

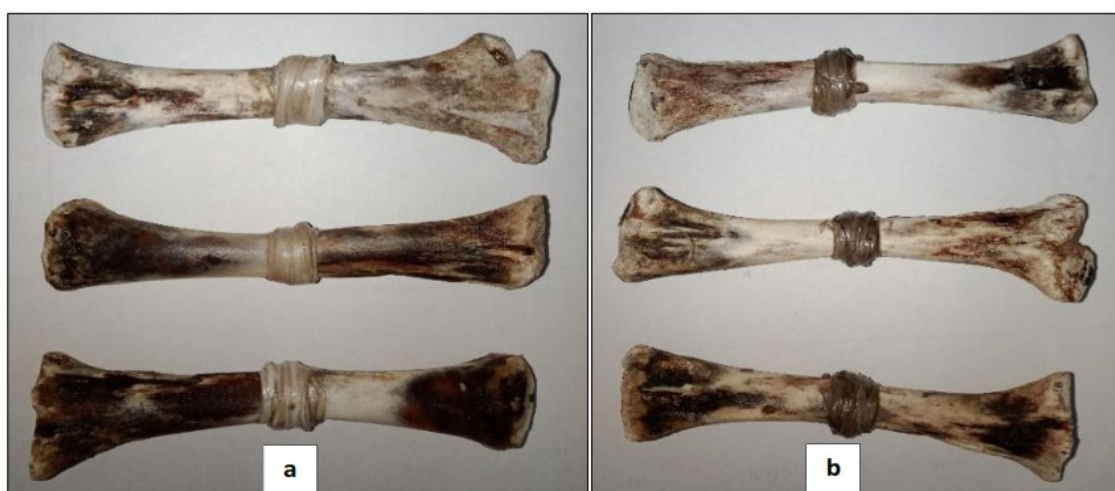


Figure 3. Chicken bones covered by (a) *E. tirucalli* latex and (b) CMs/latex composites.

The antibacterial activity of CMs and CMs/latex composites (A, B, and C) was tested against *S. aureus* bacteria using the diffusion method. The bacteria were purchased from the Medical Faculty of Universitas Gadjah Mada, Indonesia. All equipment for the antibacterial test was provided by the Microbiology laboratory, Universitas Negeri Yogyakarta, Indonesia. The DIZ was determined to identify the anti-bacterial activity of the samples. The bacterial culture was grown on nutrient agar (NA) and nutrient Broth (NB) media. The bacteria were then cultured in a medium on a petri dish. Paper disks were immersed in the sample solutions for 15 minutes, and then placed on solidified NA media and in a sterile room at 37 °C. Three petri dishes were given various samples of the paper disks, i.e., CMs (A, B, and C), *E. tirucalli* latex (2 ml, 3 ml, and 4 ml), and CMs/latex composites (A, B, and C). This test was carried out for 24 hours, with the DIZ measured every 3 hours using a caliper.

Finally, the latex and CMs/latex composites were applied to chicken bones as a simple model of treating bone fractures. This was conducted by drying and breaking the chicken bones around their middle parts. The chicken bones were then re-attached and covered (wrapped) by the latex and CMs/latex. This can be observed in Figure 3. The test on the chicken bones was conducted to determine the tensile strength of the latex and CMs/latex composites. The tensile strength test was conducted at the Faculty of Engineering, Universitas Negeri Yogyakarta using the UTM. In principle, UTM pulled the tested material until it broke. This produced the peak tensile force required to split the chicken bones wrapped by the latex and CMs/latex composites. Moreover, the tissue layers of the chicken bone without coating, chicken bone coated by CMs, and CMs/latex were also observed using a light microscope (Optilab Microscope).

3. Results and Discussion

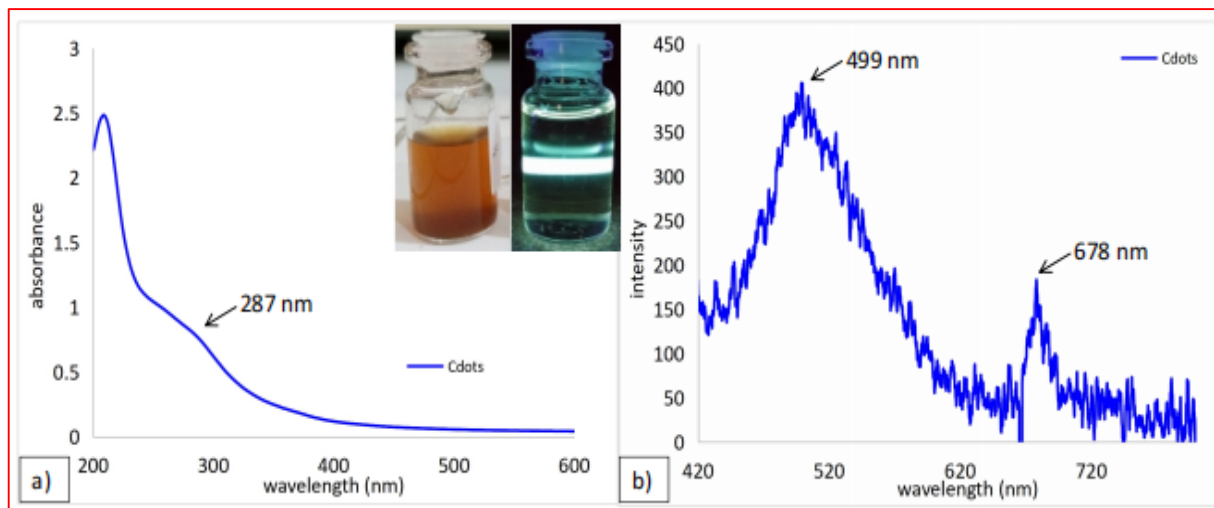


Figure 4. The (a) absorption and (b) emission spectra of the CMs.

The results of the UV-Vis and PL characterizations of the CMs are presented in Figures 4(a) and 4(b), respectively. Figure 4(a) shows an absorption peak at a wavelength of 287 nm, which is attributed to the $\pi \rightarrow \pi^*$ transition of C=C (Rahmani & Ghaemy, 2019; Mewada et al., 2015). Figure 4(b) shows two intensity peaks. The first dominant peak is at a wavelength of 499 nm, which belongs to the cyan wavelength range, i.e., 495 nm to 570 nm. This suggests that the CMs sample has a cyan luminescence in accordance with the luminescence shown in the inset of Figure 4 (right picture), which is obtained by exposing the CMs solution with a UV/violet laser (a wavelength of 405 nm). In addition to the

first dominant intensity peak, a second peak is produced at a wavelength of 678 nm. This latter wavelength belongs to the red emission spectrum, i.e., 620 nm to 750 nm. This second peak indicates the presence of *chlorophyll* in the CMs sample (Dwandaru et al., 2020; Li et al., 2017). It is possible that the *chlorophyll* from the branches of *E. tirucalli* still remains, although the branches have been heated. However, the intensity is small compared to the first intensity peak. The CMs solution has a brownish appearance under sunlight (inset Figure 4, left picture).

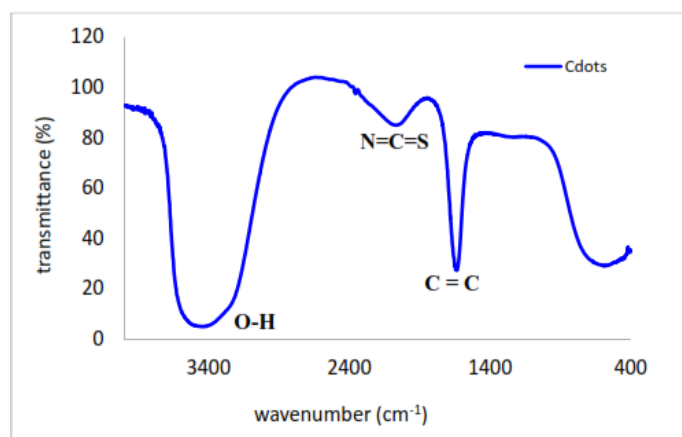


Figure 5. IR spectrum of the CMs.

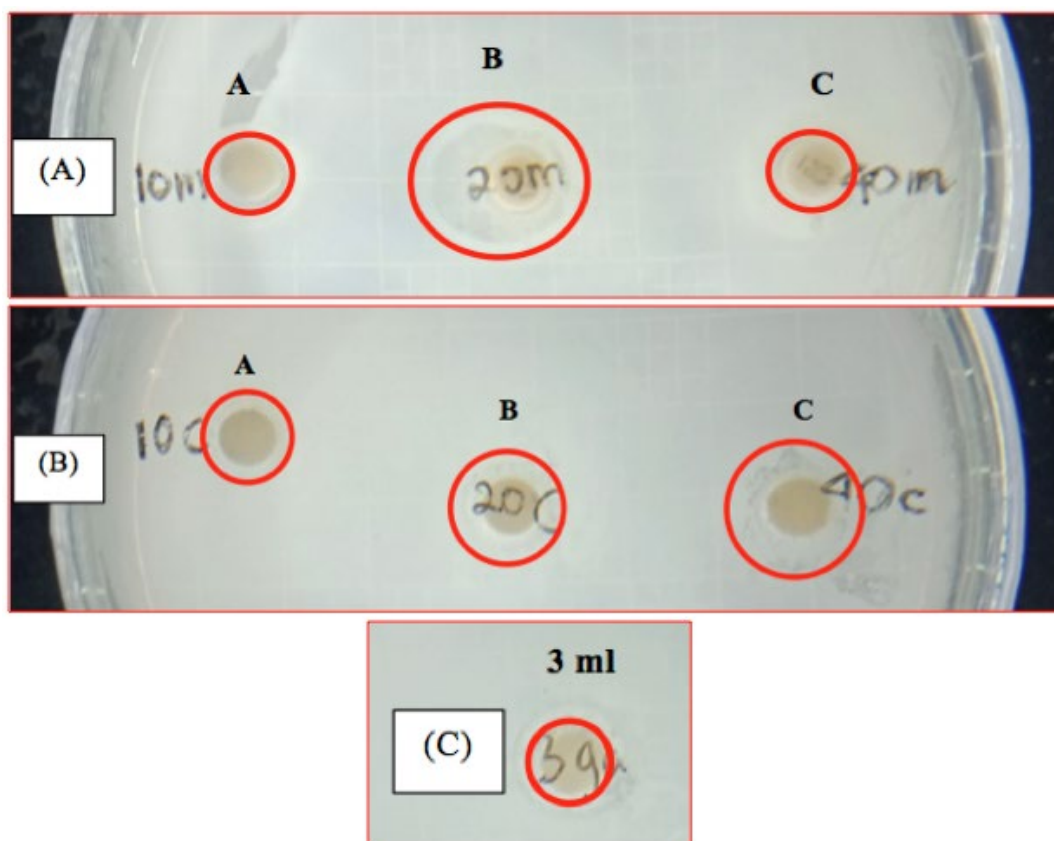


Figure 6. DIZs after 24 hours of the CMs (A), CMs/latex composites (B), and *E. tirucalli* latex (C).

The IR spectrum of the CMs is depicted in Figure 5. The FTIR spectrum shows bands of C=C, O-H, and N=C=S functional groups at 1633 cm^{-1} , 3446 cm^{-1} , and 2067 cm^{-1} , respectively. The functional group of C=C is in accordance with the UV-Vis result shown in Figure 4(a). Furthermore, the functional group of OH has a water solubility property that makes the CMs easy to conjugate with other materials, e.g., the latex.

The CMs solution was then combined with *E. tirucalli* latex to produce the CMs/latex composites. The latter has a sticky texture like glue and white color following the latex (see Figure 2).

Furthermore, higher concentrations of the CMs resulted in a thicker composite. In order to study the antibacterial property of the composites, the antibacterial tests were conducted. The antibacterial activities of the CMs and CMs/latex composites are observed against *S. aureus* by measuring the DIZ of the aforementioned samples. The DIZs after 24 hours are shown in Figure 6. The DIZs of the samples can be observed inside the red circles in the figure. The average DIZ of each sample is shown in Table 1.

Table 1. The average DIZs of the samples.

No.	CMs			Latex		CMs/latex composites	
	Sample	Average ± 0.05 (mm)		Volume (ml)	Average ± 0.05 (mm)	Sample	Average ± 0.05 (mm)
1.	A	1.44				A	1.37
2.	B	2.59		3	1.24	B	2.08
3.	C	1.90				C	3.24

It can be observed in Table 1 that the highest DIZ of 3.24 ± 0.05 mm is obtained for sample C of the CMs/latex composites consisting of 40% CMs solution. In the case of the CM/latex composites, the higher the concentration of the CMs, the higher the antibacterial activity, which is indicated by the higher DIZ results. This is expected as the composite of the two materials, i.e., CMs/latex composites, produces better antibacterial properties compared to the individual components, i.e., CMs and latex. In addition, the latex naturally has antibacterial properties

(Mali & Panchal, 2017). This is evidenced by the average DIZ obtained by the latex (3 ml) of 1.24 ± 0.05 mm.

On the other hand, the CMs samples also have antibacterial properties, with the highest DIZ of 2.59 ± 0.05 mm for sample B. All A, B, and C samples of the CMs and CMs/latex composites have higher DIZs compared to the DIZ of the pure latex. This indicates that the antibacterial property of CMs and CMs/latex composites performs better than that of pure latex. However, pure CMs of samples A and B have DIZs higher than the CMs/latex composites

of A and B, respectively. Only sample C of the CMs/latex composites has a higher DIZ compared to the pure CMs of sample C. This partially indicates that preparing composite materials of CMs/latex produces better antibacterial properties as expected. Therefore, the composite of CMs with the latex can significantly improve the antibacterial ability against *S. aureus* and can be further used as an antibacterial agent. The antibacterial properties of CMs can be extracted from the precursor of CMs, namely the branches of the *E. tirucalli* plant, which have natural antibacterial components. Furthermore, CMs are smaller in size compared to the latex. Hence, the former are more effective in inhibiting the growth of *S. aureus* bacteria (Muktha et al., 2020).

S. aureus is a gram-positive bacterium that can cause various harms to human health, particularly in this case concerning, e.g., bones and joint infections (Bouiller & David, 2023) and fracture-related infection (FRI) in orthopedic surgery (Li et al., 2023). Hence, this justifies the preparation of CMs/latex composites with antibacterial properties against *S. aureus*. For a comparison, the highest DIZ of 3.24 ± 0.05 mm of the CMs/latex composites is lower than the DIZ of CM core-shell/SiO₂ (SiO₂@C) and AgNP/Cdots nanocomposites of 6.7 mm to 11.2 mm and 9.80 mm, respectively (Khemthong et al., 2023; Wang et al., 2022). The difference in the values of the DIZ is most likely caused by the various concentrations used for each composite. Hence,

modifying the concentration of the composite's components may be conducted to increase the DIZ of the CMs/latex composites.

Moreover, we argue that the antibacterial activity of the CMs/latex composites is a synergetic mechanism between the individual components of the composites, i.e., CMs and latex. The latex is essentially a complex emulsion consisting of proteins, starches, alkaloids, sugars, and gums with sources of carbon, oxygen, nitrogen, and sulfur (Bano et al., 2018). Some of these compounds are responsible for the antibacterial activity of the latex in the form of antimicrobial compounds (AMCs) and/or antimicrobial peptides (AMPs), e.g., proteins and alkaloids. These AMCs and AMPs can penetrate the bacterial cell membranes, especially the AMPs being hydrophobic (Gracz-Bernaciak et al., 2021). On the other hand, many antimicrobial mechanisms can be attributed to the CMs, e.g., physical or mechanical destruction, oxidative stress via reactive oxygen species (ROS), and photodynamic effects (Xin et al., 2018). Hence, the synergy between CMs and latex improves the physical or mechanical penetration strength towards the bacterial cell membranes. The combination of AMCs, AMPs, and CMs produces mechanical damage to the outer membranes of *S. aureus* cell walls. The damage that is exerted upon the bacterial cell membranes depends on the contact interaction between the CMs/latex composites and *S. aureus*, depending on the dimensionalities of the composites.



Figure 7. Tensile strength test of the latex (a) and CMs/latex composites (b) wrapped on chicken bones.

A fractured chicken bone model was used to investigate the tensile strength of the latex and CMs/latex composites. The latex and CMs/latex composites are intended as an alternative to commonly used metal objects in the process of healing and/or repositioning the bone fracture. Samples of chicken bones wrapped in the latex and CMs/latex composites are shown in Figure 3. Physically, the latex covering the bone fracture has a

white color, while CMs/latex composites have a darker grey color. This color difference is due to the addition of CMs in the CMs/latex composites. The model is tested for tensile strength using the UTM. The results of the UTM tests can be seen in Figure 7. The peak tensile force of the tested chicken bones wrapped with the latex and CMs/latex composites are shown in Table 2.

Table 2. The peak tensile force of the latex and CMs/latex composites.

No.	Sample	Peak tensile force of latex ± 0.0005 (kN)	Peak tensile force of CMs/latex ± 0.0005 (kN)
1.	1	0.0110	0.0240
2.	2	0.0150	0.0250
3.	3	0.0160	0.0110
Average		0.0140	0.0200

The UTM test shows the force required to break the material. The greater the force required, the stronger the material. A strong wrapping is required to keep the fractured bones in good shape during the healing period. It may be observed in Table 2 that the highest average tensile force is obtained for the chicken bones wrapped with CMs/latex composites, with an average of 0.02 kN, while the chicken bones wrapped with latex have an average tensile strength value of 0.014 kN. This indicates that the CMs/latex composites have the ability to withstand higher tensile stress than the sample of the latex. Hence, the addition of CMs increases the strength of the latex as an alternative fracture treatment.

Finally, Figure 8 shows the images of the chicken bone layers without coating [Figure 8(a)], coated with latex [Figure 8(b)], and coated with CMs/latex composites [Figure 8(c)]. The chicken bone layer without coating clearly shows elongated fibrous surface like

threads. Hence, the texture of the surface layer appears to be uneven. On the other hand, the image of the chicken bone coated by latex shows a smooth surface, while the chicken bone coated by CMs/latex composites has a smooth and dense surface. This means that the latex and CMs/latex composites are able to cover the bone fibers. Moreover, the CMs/latex composites are able to densely cover the chicken bone layer compared to the latex. The CMs added to the latex fill in the gaps in the chicken bone layers better than the pure latex. This makes CMs/latex composites look denser and can cover the chicken bone better than the latex alone. These results also reinforce the tensile strength test results, where the chicken bone wrapped with CMs/latex composites has a greater tensile strength compared to the pure latex. Since the latex is a sticky emulsion, the addition of CMs particles makes the composites denser, hence improving the strength of the CMs/latex composites.

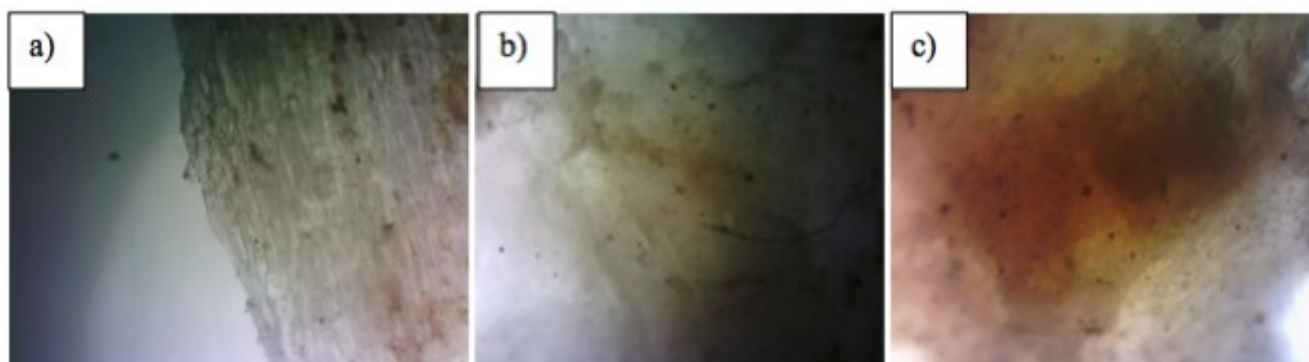


Figure 8. Images of the chicken bone layer without coating (a), coated with latex (b), and coated with CMs/latex composites (c) with a magnification of 5.3X.

4. Conclusion

The CMs were successfully prepared through heating at a low temperature from the branches of the *E. tirucalli* plant. The CMs/latex composites have the highest DIZ against *S. aureus* bacteria compared to the latex and CMs, which shows that the antibacterial ability is improved if the latex and CMs are combined. The fractured chicken bone wrapped with CMs/latex composites has the highest tensile strength because CMs/latex have a smooth and dense surface, so that they can bind the chicken bone better than the latex alone. Hence, the CMs/latex composites can be developed as an alternative for bone fracture

treatment. Further characterization of the CMs and CMs/latex composites can be conducted for future study, such as using a high-resolution transmission electron microscope (HR-TEM). Further studies can also be conducted on the application of the CMs/latex composites to various parts of the bones.

5. Acknowledgement

The authors would like to thank the Faculty of Mathematics and Natural Science, Universitas Negeri Yogyakarta, for supporting this study.

5. References

- Bajpai S K., D'Souza A., Suhail B. (2019). Carbon dots from Guar Gum: Synthesis, characterization and preliminary in vivo application in plant cells *Mater. Sci. Eng. B.* 241.
- Bano D., Kumar V., Singh V K., Chandra S., Singh D K., Yadav P K., Talat M., Hasan S H. (2019). A facile and simple strategy for the synthesis of label free carbon quantum dots from the latex of *Euphorbia mili* and its peroxidase-mimic activity for the naked eye detection of glutathione in a human blood serum *ACS Sustainable Chem. Eng.* 7: 1923.
- Bouiller K., David M Z. (2023). Staphylococcus aureus genomic analysis and outcomes in patients with bone and joint infections *Int. J. Mol. Sci.* 24(4): 3234.
- da Silva R F., Carneiro C N., do C. de Sousa C B., Gomez F J V., Espino M., Boiteux J., Fernandez M A., Silva M F., Dias F S. (2022). Sustainable extraction bioactive compounds procedures in medicinal plants based on the principles of green analytical chemistry: A review *Microchem. J.* 175: 107184.
- de Medeiros T V., Manioudakis J., Noun F., Macairan J –R., Victoria F., Naccache R. (2019). Microwave-assisted synthesis of carbon dots and their applications *J. Mater. Chem. C.* 7: 7175-7195.
- Dong X., Awak M A., Tomlinson N., Tang Y., Sun Y –P., Yang L. (2017). Antibacterial effects of carbon dots in combination with other antimicrobial reagents *PLoS One* 12: e0185324.
- Dwandaru W S B., Bilqis S M., Wisnuwijaya R I., Isnaeni (2019). Optical properties comparison of carbon nanodots synthesized from commercial granulated sugar using hydrothermal method and microwave *Mater. Res. Express.* 6: 105041.
- Dwandaru W S B., Fadli A L., Sari E K., Isnaeni (2020). Cdots and Cdots/S synthesis from nam-nam fruit (*Cynometra cauliflora* L.) via frying method using cooking oil *Dig. J. Nanomater. Biostructures.* 15: 555.
- Dwandaru W S B., Sari E K. (2020). Chicken bone wastes as precursor for C-dots in olive oil *J. Phys. Sci.* 31: 113.
- Ghosh T., Das T K., Das P., Banerji P., Das N Ch. (2022). Current scenario and recent advancement of doped carbon dots: a short review scientocracy update (2013–2022) *Carbon Lett.* (2022).
- Gracz-Bernaciak J., Mazur O., Nawrot R. (2021). Functional studies of plant Latex as a rich source of bioactive compounds: focus on proteins and alkaloids *Int. J. Mol. Sci.* 22(22): 1242.
- Kaur P., Verma G. (2022). Converting fruit waste into carbon dots for bioimaging applications *Mater. Today Sustain.* 18: 100137.
- Khajuria D K., Kumar V B., Gigi D., Gedanken A., Karasik D. (2018). Accelerated bone regeneration by nitrogen-doped carbon dots functionalized with hydroxyapatite nanoparticles *ACS Appl. Mater. Interfaces.* 10: 19373.
- Khemthong P., Phanthasri J., Youngjan S., Wanmolee W., Samun Y., Sosa N., Runnim C., Kraithong W., Sangkhun W., Panthong J., Butburee T., Thanee K., Nakajima H., Supruangnet R., Towiwat P., Chanvorachote P., Sukrong S. (2023). Effect of the ethanol-to-water ratio on the properties of silica-carbon core-shell materials for prolonged antibacterial activity of thymol *Applied Surface Science* 635: 157716.
- Li J., Leung S S Y., Chung Y L., Chow S K H., Alt V., Rupp M., Brochhause C., Chui C S., Ip M., Cheung W-H., Wong R M Y. (2023). Hydrogel delivery of DNase I and liposomal vancomycin to eradicate fracture-related ethicillin-resistant staphylococcus aureus infection and support osteoporotic fracture healing *Acta Biomaterialia* 164: 223.
- Li L., Zhang R., Lu C., Sun J., Wang L., Qu B., Li T., Liu Y., Li S. (2017). In situ synthesis of NIR-Light emission carbon dots derived from spinach for bio-imaging application *J. Mater. Chem. B.* 5: 7328.
- Liu J., Li R., Yang B. (2020). Carbon dots: a new type of carbon-based nanomaterial with wide applications *ACS Cent. Sci.* 12: 2179.
- Liu X., Pang J., Xu F., Zhang X. (2016). Simple approach to synthesize amino-functionalized carbon dots by carbonization of chitosan *Sci. Rep.* 6: 31100.
- Mali P Y., Panchal S S. (2017). Euphorbia tirucalli L.: Review on morphology, medicinal uses, phytochemistry and pharmacological activities *Asian Pac. J. Trop. Med.* 7: 603.
- Maver T., Maver U., Kleinschek K S., Smrke D M., Kreft S. (2015). A review of herbal medicines in wound healing *Int. J. Dermatol.* 54: 740-751.
- Mewada A., Vishwakarma R., Patil B., Phadke C., Kalita G., Sharon M., Sharon M. (2015). Non-blinking dendritic crystals from C-dot solution *Carbon Lett.* 16: 211.
- Muktha H., Sharath R., Kottam N., Smrithi S P., Samrat K., Ankitha P. (2020). Green synthesis of carbon dots and evaluation of its pharmacological activities *BioNanoSci.* 10: 731.
- Pallavali R R., Avula S., Degati V L., Penubala M., Damu A G., Durbaka V R P. (2019). Data of antibacterial activity of plant leaves crude extract on bacterial isolates of wound infections *Data in Brief* 24: 103896.
- Pires N R., Santos C M W., Sousa R R., de Paula R C M., Cunha P L R., Feitosa J P A. (2015). Novel and fast microwave-assisted

synthesis of carbon quantum dots from raw cashew gum *J. Braz. Chem. Soc.* 26: 1274.

Rahmani Z., Ghaemy M. (2019). One-step hydrothermal-assisted synthesis of highly fluorescent N-doped carbon dots from gum tragacanth: luminescent stability and sensitive probe for Au³⁺ ions *Opt. Mater.* 97.

Sabzehmeidani M M., Mahnaee S., Ghaedi M., Heidari H., Roy V A L. (2021). Carbon based materials: a review of adsorbents for inorganic and organic compounds *Mater. Adv.* 2: 598.

Shao D., Lu M., Xu D., Zheng X., Pan Y., Song Y., Xu J., Li M., Zhang M., Li J., Chi G., Chen L., Yang B. (2017). Carbon dots for tracking and promoting osteogenic differentiation of mesenchymal stem cells *Biomater. Sci.* 5: 1820.

Sreenath P R., Mandal S., Panigrahi H., Das P., Kumar K D. (2020). Carbon dots: fluorescence active, covalently conjugated and strong reinforcing nanofiller for polymer latex *Nano-Struct. Nano-Objects.* 23: 100477.

Thakur M., Pandey S., Mewada A., Patil V., Khade M., Goshi E., Sharon M. (2014). Antibiotic conjugated fluorescent carbon dots as a theranostic agent for controlled drug release, bioimaging, and enhanced antimicrobial activity *J. Drug Deliv.* 2014.

Wang P., Song Y., Mei Q., Dong W-F., Li L. (2022). Silver nanoparticles@carbon dots for synergistic antibacterial activity *Applied Surface Science* 600: 154125.

Wang Y H., Hu A. (2017). Carbon quantum dots: synthesis, properties and applications *J. Mater. Chem. C.* 2: 6921.

Weber K., Quicker P. (2018). Properties of biochar *Fuel* 217: 240.

Xia C., Zhu S., Feng T., Yang M., Yang B. (2019). Evolution and synthesis of carbon dots: from carbon dots to carbonized polymer dots *Adv. Sci.* 6: 1901316.

Xin Q., Shah H., Nawaz A., Xie W., Akram M Z., Batool A., Tian L., Jan S U., Boddula R., Guo B., Liu Q., Gong J R. (2018). Antibacterial carbon-based nanomaterials *Adv. Mater.* 2018: 1-15.

Zhai X., Zhang P., Liu C., Bai T., Li W., Dai L., Liu W. (2012). Highly luminescent carbon nanodots by microwave-assisted pyrolysis *Chem. Commun.* 48: 7955.